AD_____

Award Number: W81XWH-05-1-0492

TITLE: An in Vitro Study of Breast Cancer Invasion into the Lymphatics

PRINCIPAL INVESTIGATOR: Melody Swartz, Ph.D.
Jacqueline Shields, Ph.D.

CONTRACTING ORGANIZATION: Ecole Polytechnique Federale de Lausanne
Lausanne CH 1015
Switzerland

REPORT DATE: August 2006

TYPE OF REPORT: Final

PREPARED FOR: U.S. Army Medical Research and Materiel Command
Fort Detrick, Maryland 21702-5012

REPORT DOCUMENTATION PAGE

Form Approved
OMB No. 0704-0188

1. REPORT DATE *(DD-MM-YYYY)*	2. REPORT TYPE	3. DATES COVERED *(From - To)*
01/08/06	Final	25 Jul 05 – 24 Jul 06

4. TITLE AND SUBTITLE
An in Vitro Study of Breast Cancer Invasion into the Lymphatics

5a. CONTRACT NUMBER

5b. GRANT NUMBER
W81XWH-05-1-0492

5c. PROGRAM ELEMENT NUMBER

6. AUTHOR(S)
Prof. Melody Swartz, Ph.D.; Jacqueline Shields, Ph.D.

E-Mail: melody.swartz@epfl.ch

5d. PROJECT NUMBER

5e. TASK NUMBER

5f. WORK UNIT NUMBER

7. PERFORMING ORGANIZATION NAME(S) AND ADDRESS(ES)

Ecole Polytechnique Federale de Lausanne
Lausanne CH 1015
Switzerland

8. PERFORMING ORGANIZATION REPORT NUMBER

9. SPONSORING / MONITORING AGENCY NAME(S) AND ADDRESS(ES)
U.S. Army Medical Research and Materiel Command
Fort Detrick, Maryland 21702-5012

10. SPONSOR/MONITOR'S ACRONYM(S)

11. SPONSOR/MONITOR'S REPORT NUMBER(S)

12. DISTRIBUTION / AVAILABILITY STATEMENT
Approved for Public Release; Distribution Unlimited

13. SUPPLEMENTARY NOTES

14. ABSTRACT
None provided.

15. SUBJECT TERMS
Lymphatic, CCL21, CCR7, interstitial flow, chemotaxis

16. SECURITY CLASSIFICATION OF:			17. LIMITATION OF ABSTRACT	18. NUMBER OF PAGES	19a. NAME OF RESPONSIBLE PERSON
a. REPORT	b. ABSTRACT	c. THIS PAGE			USAMRMC
U	U	U	UU	44	19b. TELEPHONE NUMBER *(include area code)*

Standard Form 298 (Rev. 8-98)
Prescribed by ANSI Std. Z39.18

Table of Contents

Introduction……..4

Body……4

Key Research Accomplishments……8

Reportable Outcomes…… 8

Conclusions……8

References……8

APPENDICES……9

INTRODUCTION

Lymphatic metastasis is a major prognostic factor for breast cancer patients. Despite its importance, the mechanisms underlying lymphatic metastasis are poorly understood and the question of how cancer cells access the lymphatics – i.e. whether they primarily induce lymphangiogenesis (sprouting of new lymphatic vessels) or invade preexisting lymphatics – is debated in the literature. We challenge the notion of tumor lymphangiogenesis as the major mechanism for tumor entry into the lymphatics and suggest that the biophysical and biochemical factors induced or produced by the tumor, including VEGF-C, act to promote tumor cell migration towards lymphatics, not vice-versa. In real mammary carcinomas (as opposed to subcutaneously xenografted), blood vessels are leaky, interstitial fluid pressure is high, and fluid exudes from the tissue into the surrounding stroma and eventually into the lymphatics. This biophysical environment promotes the transport of any tumor-secreted factors, including VEGF-C, *from* the tumor *towards* the lymphatics. In light of these factors, we hypothesized that tumor-secreted factors can be delivered to the lymphatics by natural biophysical forces, where it stimulates the production of tumor cytokines by the "activated" lymphatics, in turn promoting tumor cell invasion into surrounding lymphatics. In this one-year project, we proposed to first develop a novel tissue engineered tumor extracellular matrix (ECM)-lymphatic environment and then use it to answer questions relating to this novel hypothesis.

BODY

The submitted proposal outlined the following tasks to investigate:

Task 1 – Develop a 3D *in vitro* co-culture system for breast tumor-lymphatic interactions to facilitate our proposed *in vitro* studies. This model will introduce environmental factors including extracellular matrix components and interstitial flow, which are not accounted for in current systems and will therefore allow us to accurately examine cell – cell interactions in a more controlled and physiologically relevant environment.

a) Develop and optimize a method to co-culture the two cell types (mammary carcinoma cells and lymphatic endothelial cells, or LECs) within a fibrin gel in a device optimized for confocal microscopy

b) Determine the relative migratory capacities of breast cancer cells and lymphatic endothelial cells within the gel preparation

c) Asses the roles of extracellular matrix components and low interststial flow on tumor cell-lymphatic communication/signaling and migratory pathways

Task 2 – Determine the extent to which lymphatic endothelial cells induce tumor cell migration and adhesion via VEGF-C-stimulated chemokines. We will specifically test the hypothesis that VEGF-C induces CCL21 upregulation in lymphatic endothelial cells, which in turn attracts tumor cells and also upregulates Mannose Receptor on lymphatic endothelial cells promoting tumor cell adhesion. This introduces a new mechanism whereby VEGF-C overexpression by tumors causes increased metastasis, without necessarily inducing lymphangiogenesis, as current dogma dictates. In addition, it would pinpoint potential new targets for anti-metastasis therapeutic strategies. We foresee continuing investigations on other potential tumor-induced, lymphatic-derived chemokines and adhesion molecules that may facilitate tumor invasion into lymphatics after these initial studies are completed.

a) Using the same *in vitro* assays as described, in the presence of inhibitors (including blocking antibodies to anti-VEGFR-3 and CCL21 and siRNAs for VEGF-C and CCL21 to determine their roles in lymphatic-tumor crosstalk

b) Assess whether tumor-derived VEGF-C affects the expression of adhesion molecules (e.g. mannose receptor) on lymphatic endothelial cells promoting tumor cell adhesion to lymphatics using Western blottting and immunostaining

During the funded period, we accomplished nearly all of the proposed tasks. The outcomes of this preliminary project have been presented to and received by scientific peers with enthusiasm and has spawned new research projects in our laboratory. The major outcome of this research project is the first experimental evidence of a new mechanism of tumor cell invasion into the lymphatics – one that is autocrine driven, when interstitial flow is present – which we have termed autologous chemotaxis. Autologous chemotaxis has the potential to significantly impact the field of cancer research but has broader implications for the fields of immune cell trafficking other cells under the influence of interstitial flow.

In human mammary carcinomas, blood vessels are leaky, interstitial fluid pressure is high, and fluid exudes from the tissue into the surrounding stroma and eventually into the lymphatics. This biophysical environment promotes the transport of any tumor-secreted factors, including growth factors and chemokines, *from* the tumor *towards* the lymphatics. Furthermore, the chemokine receptor CCR7 (receptor for CCL19 and 21), normally involved in immune cell trafficking has consistently been linked to lymph node metastasis in clinical studies, although the mechanisms behind these observations are not understood (Gunther et al., 2005; Heresi et al., 2005). In light of these factors, we hypothesized that tumor-secreted factors (possibly hijacked from the immune system) can be delivered to the lymphatics by natural biophysical forces, where they stimulate the production of tumor cytokines by the "activated" lymphatics, in turn promoting tumor cell invasion into surrounding lymphatics.

To investigate this hypothesis, we first needed to implement and test a relevant *in vitro* model of the tumor-ECM-lymphatic microenvironment. The biophysical environment that are encountered by most cells, including tumor cells and lymphatics have to date been neglected by current *in vitro* and to some extent, *in vivo* experimental strategies. Our new model incorporated tumor cells, ECM, lymphatic endothelial cells and interstitial flow to recapitulate the key features of such an environment within a modified Boyden chamber assay. This well characterized assay was modified in such a way as to be able to incorporate tumor cells suspended within a thin 3-dimensional matrix. For the purpose of this study, Growth Factor Reduced Matrigel was deemed most suitable due to its proteoglycans content since the chemokines of interest readily bind heparan sulfate proteoglycans and become immobilized within the matrix. We have also been able to seed LECs onto the underside of the membrane to represent the matrix-lymphatic boundary. Most significantly to our hypothesis, were we subsequently able to add directional physiologic levels of interstitial flow through the cell-gel compartment (Figure 1). More experimental details can found in the appended manuscript submission.

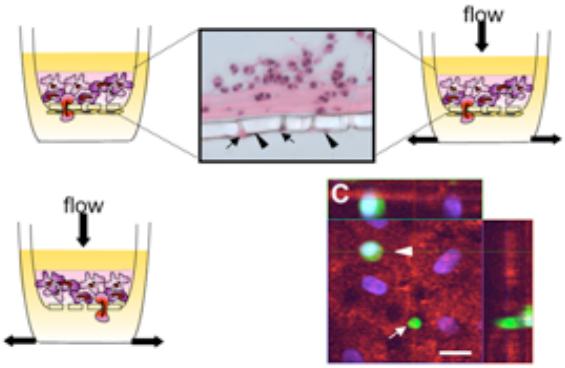

Figure 1

Under static conditions, the presence of LECs stimulated enhanced migration of tumor cells compared to tumor cells alone (LECs did not migrate through a 3D matrix). Therefore it was assumed that some and cross-talk occurred between the two cells types. Significantly, when CCR7 was blocked migration was attenuated suggesting that LECs stimulated tumor cell migration via reciprocal paracrine CCL21/19 signaling pathways.

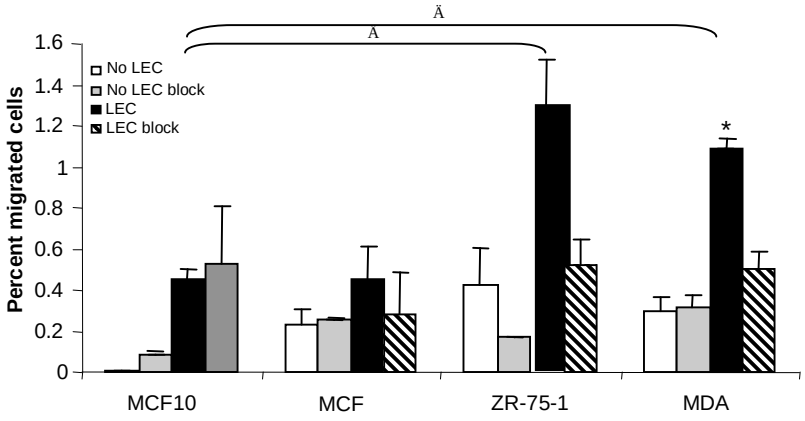

Figure 2

Lymphatic endothelial cells and tumor cells were then characterized for chemokine expression to ensure that the observations were indeed CCL21-dependent. Surprisingly, expression profiles were strongly dependent on the culture environment (2D vs. 3D). To perform a more comprehensive study, a panel of normal and breast cancer cell lines with differing metastatic potentials were assessed. These included MCF10a (normal mammary epithelial cell line) and three breast cancer cell lines, MCF7, ZR-75-1 and MDA-MB-435S (listed in order of increasing metastatic potential). Cells maintained in 2D, as typically used in most experiments to date, did not produce detectable levels of CCL21 or CCL19 (the ligands of CCR7). However, when cultured in a more relevant 3D matrix, LECs produced significant amounts of both chemokines. More surprisingly, tumor cells but not normal mammary epithelial cells also produced these chemokines. Tumor cells also expressed CCR7. A simple 3D migration assay further demonstrated that tumor cells were responsive to CCL21 and were able to migrate up a CCL21 gradient much more readily than normal mammary cells confirming that the CCR7 detected on these cells was indeed functional. These surprise findings spawned the question of whether tumor cells could possibly secrete and utilize their own autocrine source of CCR7 ligand to reach local lymphatics. Under static conditions this autocrine phenomenon would not be of relevance but the fact that interstitial flow is always directed from a tumor to the draining lymphatic could effectively bias the distribution of autocrine chemokine in such a way that a cell is able to detect a concentration gradient to migrate along. To investigate this autocrine phenomenon, we used the described system in the absence of lymphatic endothelial cells but in the presence of slow interstitial flow. This allowed us to specifically determine any tumor-flow mediated effects.

Figure 3 shows evidence in support of our hypothesis: namely that low levels of interstitial flow induced invasive migration through a 3D matrix. The degree of response, however, differed with cell type with the breast cancer cell lines producing a much more robust migration in response to interstitial flow than normal cells. This pattern correlated with the metastatic potential of cells tested. If the responses observed were indeed mediated autocrine CCR7 signaling then neutralization of the receptor would prevent flow induced migration hence the experiments were repeated in the presence of blocking antibody cocktail against CCL21 and CCR7. Migration responses of normal mammary epithelial cells to flow were not mediated by CCR7 signaling as neutralization had no effect. MCF10 migration was a result of flow induced directed proteolysis as the pan MMP inhibitor GM6001 abolished all responses. In contrast, those migration responses observed in the breast cancer cells (MCF7, ZR-71-1 and MDA-MB-435S) were significantly inhibited when CCR7 signaling was prevented. This demonstrated that flow-enhanced migration was indeed a chemotactic phenomena, yet autologous. We have termed this new, novel lymphangiogenesis-independent mechanism of tumor cell homing to lymphatics “autologous chemotaxis”, and this data represents the first experimental evidence.

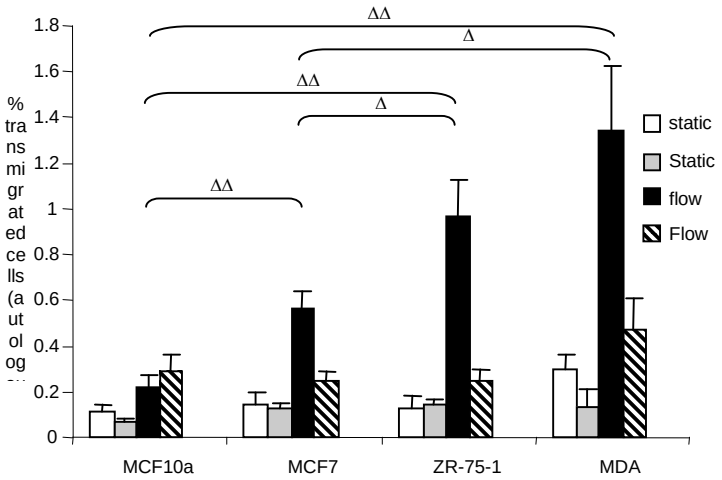

Figure 3.

When all biophysical parameters were combined, that is LECs, tumor cells, matrix and interstitial flow migration responses to either LECs (paracrine signaling) or interstitial flow (autocrine) were further augmented as the factors acted in synergy (Fig. 4). Computational modeling (not shown) were consistent with these behaviors (see attached manuscript).

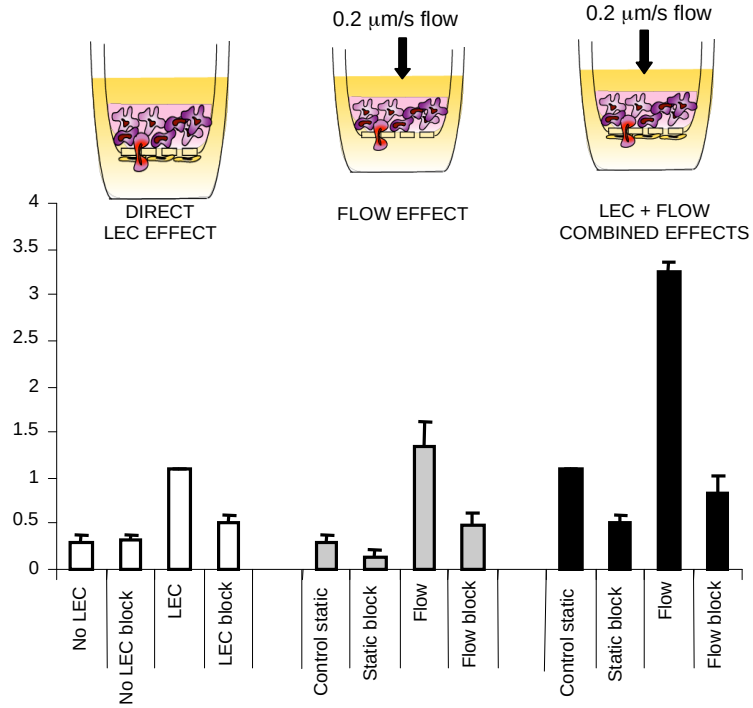

Figure 4.

Furthermore, VEGF-C, the primary lymphangiogenic growth factor has also been correlated with lymph node metastasis in animal studies and *in vitro* studies (Mandriota et al., 2001; Skobe et al., 2001), however the need for lymphangiogenesis in human tumors remains controversial (Wong et al., 2005). So if VEGF-C does mediate lymphatic metastasis it is possible that it plays an alternative non-lymphangiogenic role (and indeed, LECs cannot migrate through a 3D matrix). We have begun to investigate the combined roles of VEGF-C and CCL21 in lymphatic homing and we have preliminary data (as assessed by ELISA) to suggest that VEGF-C can upregulate CCL21 secretion by LECs. This may be significant to the overall lymphatic homing hypothesis i.e. that VEGF-C may also be transported by interstitial flow to subsequently act or peripheral lymphatics further propagating chemical signals. We therefore suggest, from our current findings that autologous chemotaxis is the driving force of lymphatic homing and guides tumor cells in the direction of functional lymphatics when too far away to detect lymphatic signals. VEGF-C stimulated lymphatic signals are subject to the negative convective forces created by interstitial flow which limit the broadcast distance but these signals may act to

amplify the autologous gradient and further guide tumor cells to lymphatic surface when they reach close proximity to the vessel. VEGF-C may in turn have direct effects on both tumor cells and LECs by regulating molecular expression to allow transmigration. This task remains to be investigated and could not be completed within the funding period.

KEY RESEARCH ACCOMPLISHMENTS

- Development of a reproducible *in vitro* model that captures multiple aspects of the tumor-lymphatic microenvironment, including interstitial flow
- First evidence that when cultured in 3D environments, invasive tumor cells secrete autocrine CCR7 ligands, and that secretion correlates with invasiveness
- First experimental evidence of "autologous chemotaxis" by tumor cells as promoted by the surrounding biophysical forces to home to lymphatics without necessarily requiring lymphatic signaling
- Paracrine signals from the lymphatic vessels can combine with autocrine signals from the tumor cell to augment chemokine gradients and enhance invasion of tumor cells towards lymphatics

REPORTABLE OUTCOMES

- Manuscript submitted to Cancer Cell, a high impact peer reviewed journal
- Manuscript in preparation with a collaborating PhD student
- Posters and oral presentations at conferences attended by peers including: Gordon research conference on Molecular Mechanisms in Lymphatic Biology, Biomedical Engineering Society Annual Meeting, Annual meeting of the European Microcirculation Society, and the international meeting "Cancer Invasion and Metastasis" in Switzerland
- From this work we will apply for further funding from the NIH, Swiss National Science Foundation, and Department of Defense Breast Cancer Research Program (Innovator Award).

CONCLUSIONS

Funding from the D.o.D. enabled a preliminary albeit foundational study to commence. We have provided experimental evidence in support of our original hypothesis of tumor-LEC paracrine communication but have also identified an additional facet that is significant and complementary to our concept hence we spent time investigating this observation more thoroughly. We have been able to determine that tumor cells have exploit normal physiological processes found in immune cell homing having evolved to secrete and use autologous sources of lymphatic homing chemokines CCL21 and CCL19 in a process we have termed autologous chemotaxis. The findings of this study have stimulated much discussion and have lead to the development of further more in depth projects within this laboratory. The phenomenon of autologous chemotaxis stands to impact the field of cancer research by means of targets for anti-metastasis therapies but also its broad appeal has significant implication to the field of immune cell trafficking as well as all areas of research into cells under the influence of interstitial flow. To more comprehensively investigate this mechanism we are aiming to develop an in vivo model to determine the relative roles of autocrine versus paracrine signaling and their individual impacts on metastasis.

REFERENCES

Chary, S. R., and Jain, R. K. (1989). Direct measurement of interstitial convection and diffusion of albumin in normal and neoplastic tissues by fluorescence photobleaching. Proc Natl Acad Sci U S A 86, 5385-5389.

Dafni, H., Israely, T., Bhujwalla, Z. M., Benjamin, L. E., and Neeman, M. (2002). Overexpression of vascular endothelial growth factor 165 drives peritumor interstitial convection and induces lymphatic drain: magnetic

resonance imaging, confocal microscopy, and histological tracking of triple-labeled albumin. Cancer Res *62*, 6731-6739.

Gunther, K., Leier, J., Henning, G., Dimmler, A., Weissbach, R., Hohenberger, W., and Forster, R. (2005). Prediction of lymph node metastasis in colorectal carcinoma by expressionof chemokine receptor CCR7. Int J Cancer *116*, 726-733.

Heresi, G. A., Wang, J., Taichman, R., Chirinos, J. A., Regalado, J. J., Lichtstein, D. M., and Rosenblatt, J. D. (2005). Expression of the chemokine receptor CCR7 in prostate cancer presenting with generalized lymphadenopathy: report of a case, review of the literature, and analysis of chemokine receptor expression. Urol Oncol *23*, 261-267.

Mandriota, S. J., Jussila, L., Jeltsch, M., Compagni, A., Baetens, D., Prevo, R., Banerji, S., Huarte, J., Montesano, R., Jackson, D. G., *et al.* (2001). Vascular endothelial growth factor-C-mediated lymphangiogenesis promotes tumour metastasis. EMBO J *20*, 672-682.

Skobe, M., Hawighorst, T., Jackson, D. G., Prevo, R., Janes, L., Velasco, P., Riccardi, L., Alitalo, K., Claffey, K., and Detmar, M. (2001). Induction of tumor lymphangiogenesis by VEGF-C promotes breast cancer metastasis. Nature Med *7*, 192-198.

Wong, S. Y., Haack, H., Crowley, D., Barry, M., Bronson, R. T., and Hynes, R. O. (2005). Tumor-secreted vascular endothelial growth factor-C is necessary for prostate cancer lymphangiogenesis, but lymphangiogenesis is unnecessary for lymph node metastasis. Cancer Res *65*, 9789-9798.

APPENDICES

MANUSCRIPT ATTACHED (submitted to Cancer Cell; currently in 2nd review)

Autologous Chemotaxis as a Mechanism of Tumor Cell Homing to Lymphatics via Interstitial Flow and Autocrine CCR7 Signaling

Jacqueline D. Shields[1*], Mark E. Fleury[1*], Carolyn Yong[1], Alice A. Tomei[1], Gwendalyn J. Randolph[2], Melody A. Swartz[1]

1: Institute of Bioengineering, École Polytechnique Fédérale de Lausanne (EPFL), Switzerland
2: Dept. Of Gene and Cell Medicine, Icahn Research Institute, Mount Sinai School of Medicine, New York, NY 10029 USA
*these authors contributed equally

Address for Correspondence:
Melody A. Swartz
Institute of Bioengineering
School of Life Sciences / LMBM / Station 15
École Polytechnique Fédérale de Lausanne (EPFL)
1015 Lausanne, Switzerland

ph: (41) 21-693-9686
Fax: (41) 21-693-1660
Email: melody.swartz@epfl.ch

Running Title: Autologous chemotaxis of tumor cells to lymphatics

Key words: microenvironment, metastasis, in vitro, 3D, CCL21, mammary carcinoma

Summary

CCR7 chemokine receptor signaling is implicated in lymph node metastasis of many cancers, but its role is obscure. We report here a novel mechanism explaining how autocrine CCR7-mediated signaling can direct tumor cell migration towards draining lymphatics in addition to paracrine CCL21 signaling by lymphatics. Under static conditions, lymphatic endothelium induced CCR7-dependent chemotaxis of co-cultured tumor cells through a 3D matrix. However, robust increases in CCR7-dependent tumor cell migration also occurred in the presence of interstitial flow that, strikingly, could be lymphatic endothelium-independent. Instead, tumor cell-secreted chemokine promoted autologous chemotaxis in the flow direction, and this correlated with metastatic potential in four different cell lines. Computational modeling estimated that small transcellular gradients of CCR7 ligand were created under flow to drive this response, and that a greater chemotactic gradient could be induced by the combination of flow and paracrine signaling than with paracrine signaling alone. This work reveals the first evidence of autologous chemotaxis and illustrates how tumor cells may be guided toward functional draining lymphatics during metastasis.

Significance

Many cancers spread via the lymphatics but the mechanisms used by tumor cells to access lymphatics remain unclear, although expression of the chemokine receptor CCR7 has been correlated with lymph node metastasis. Using a novel 3D culture model, we provide evidence that lymphatics chemoattract CCR7-expressing tumor cells, and moreover, that physiologic levels of interstitial flow strongly enhance tumor cell migration. We show how tumor cells can utilize interstitial flow to create and amplify autologous chemokine gradients, and thus chemotact

towards the draining lymphatic even without chemotactic signals from the lymphatic. This work also provides a novel twist to the well-described phenomenon of chemotaxis by showing that a cell can receive directional cues while at the same time being the source of such cues.

Introduction

Although lymphatic metastasis is the major route of dissemination for many cancers including breast, skin, colorectal and prostate cancers (Chambers et al., 2002; Nathanson, 2003; Van Trappen and Pepper, 2002; Weigelt et al., 2005), the mechanisms governing tumor cell entry into lymphatics are not clear. It has been suggested that more aggressive tumors induce lymphangiogenesis via secretion of lymphangiogenic growth factors (He et al., 2005; Mandriota et al., 2001; Skobe et al., 2001; Stacker et al., 2001), although evidence for tumor lymphangiogenesis, or the necessity of lymphangiogenesis for lymphatic metastasis, in human cancer remains controversial (Wong et al., 2005; Clarijs et al., 2001; Sipos et al., 2005; Williams et al., 2003).

Consistently, however, lymph node metastasis has been correlated with tumor expression of certain chemokine receptors, particularly CCR7 and CRCX4 (Arya et al., 2004; Darash-Yahana et al., 2004; Kimsey et al., 2004; Patel et al., 2001; Takeuchi et al., 2004; Muller et al., 2001; Nathanson, 2003). CCR7 is of particular interest since memory CD4+ T cells and antigen-presenting dendritic cells, which constitutively traffic through the lymphatics, require CCR7 for migration to lymph nodes (Debes et al., 2005; Forster et al., 1999; Ohl et al., 2004; Randolph et al., 2005). Cancer cells may exploit similar mechanisms to access the lymphatics: indeed, CCR7 expression directly correlated to incidence of lymph node metastasis in breast (Cabioglu et al., 2005), colorectal (Gunther et al., 2005), head and neck (Wang et al., 2005), prostate (Heresi et al., 2005), non-small lung cancer (Takanami, 2003), esophageal squamous cell carcinoma (Ding et al., 2003), gastric (Mashino et al., 2002) and skin (Murakami et al., 2004; Wiley et al., 2001) cancers. The known ligands for CCR7 are CCL21 (also called SLC and 6cKine) and CCL19. CCL21 is expressed by lymphatic vessels (Gunn et al., 1998), but available evidence is

inconsistent with the notion that lymphatic vessel-derived CCL21 alone controls immune cell migration (Randolph et al., 2005). CCL21 is secreted as a 12kDa protein, but readily immobilized within extracellular matrix (ECM) and on the surface of endothelium by binding to sulfated proteoglycans (Patel et al., 2001; Handel et al., 2005). Similarly, CCL19 is secreted as an 8.8kDa protein, and is required for immunological functions including T cell priming and dendrite production by antigen presenting cells thereby affecting migratory properties.

We suggest here a novel mechanism for CCR7 ligand-mediated tumor cell chemotaxis to lymphatics. In addition to sensing a chemotactic gradient from lymphatic vessels, we propose that tumor cells can also generate autologous gradients of CCR7 ligands by secreting them into the ECM under the influence of slow interstitial flow (IF). This novel mechanism uses the drainage function of lymphatics to direct tumor cells in a chemotactic manner towards vessels serving the tumor. This mechanism also promotes more robust chemotaxis toward functional, rather than non-functional, lymphatic vessels: while both may secrete CCL21, interstitial flow will only be directed towards functional vessels. Furthermore, it is well-established that many tumors are highly vascularized, and contain abnormally leaky capillaries (Jain, 2003; Jain, 2005; Carmeliet, 2003); thus tumor fluid flows through the interstitial space towards their draining lymphatics with a velocity of 0.1-0.8μm/s (Chary and Jain, 1989; Dafni et al., 2002). This proposed mechanism follows from our recent computational demonstration that transcellular gradients of autocrine secreted morphogen can form under conditions of low interstitial flow (Fleury et al., 2006; Helm et al., 2005) in a 3D environment when the morphogen is matrix-binding. The microenvironment created by normal lymphatic functioning in the space between the tumor margin and lymphatic vessel may also, in this way, facilitate tumor migration towards lymphatics (Fig. 1A).

We use a simple and unique *in vitro* 3D culture model to mimic this biophysical microenvironment and explore the interplay between interstitial flow and chemokine signaling between tumor cells and lymphatic endothelial cells (LECs) (Fig. 1B). Matrigel, a basement membrane-like reconstituted ECM that is rich in heparan sulfate proteoglycans (Kleinman and Martin, 2005), was used to facilitate chemokine interactions with the ECM and allow pericellular gradients of both tumor-secreted and potentially LEC-secreted CCL21, which binds to sulfated proteoglycans (Patel et al., 2001, Handel et al., 2005), to be established as they would *in vivo*. We show, using 4 different transformed human mammary epithelial cell lines, that tumor cells can create autocrine gradients of CCR7 ligands that guide their chemotaxis in the direction of flow (i.e., towards functional lymphatics). This occurs when a physiologic level of interstitial flow is present, even if LECs are absent. These findings introduce a new mechanism that we have termed "autologous chemotaxis" for guiding tumor cells towards functional draining lymphatics. It also gives mechanistic insight into why CCR7 expression is strongly correlated to lymph node metastasis of tumors and suggests that CCR7 ligand secretion by tumor cells themselves, rather than, or in addition to secretion by lymphatics, may be a potential target for preventing metastatic spread.

Results

Tumor expression of CCR7 and response to CCL21 gradients

We examined a panel of 4 human breast epithelial cell lines for the presence and functional response of CCR7 which included one non-tumorigenic cell line, MCF10A (Soule et al., 1990), and 3 tumor cell lines: MCF7 (Soule et al., 1973), ZR-75-1 (Engel et al., 1978) and MDA-MB-435S (Cailleau et al., 1978). Immunofluorescence (Fig. 2A) demonstrated strong receptor

expression in the three tumor cell lines, but weak staining in LECs and the benign cell line; this was confirmed by Western blot (Fig. 2B-C).

To verify their chemotactic response to CCR7 ligand, the cells were embedded within a 1 mm thick 3D matrigel matrix, and exposed to a gradient of CCL21 protein. This CCL21 gradient stimulated chemotaxis of all three tumor cell lines tested but had no significant effect on MCF10A cells (Figs. 2D-H), as expected since it showed minimal evidence of CCR7 expression. Furthermore, co-neutralization of CCL21 and CCR7 caused a significant and almost complete inhibition of invasive migration in response to CCL21. Thus, tumor cell expression of CCR7 correlated qualitatively with their chemotactic response to a CCL21 gradient.

Tumor cells secrete autocrine CCR7 ligands

We found that all tested mammary epithelial cell lines secreted CCL19 and CCL21, ligands for the CCR7 receptor (Fig. 3A-C). The more highly invasive cell lines (MDA-MB-435S and ZR-75-1) secreted more CCR7 ligands than did the benign cell line MCF10A or the LECs. The fact that CCL21/19 secretion was higher in invasive vs. benign cell lines suggested that tumor cells may utilize autocrine CCR7 signaling mechanisms for invasion.

Of note, tumor cell secretion of both CCL19 and CCL21 was significantly higher in 3D than 2D culture conditions (Fig. 3D). The majority of protein was found within the matrigel matrix fraction for both CCL21 and CCL19 rather than within conditioned media or cell lysates, consistent with their known binding properties to sulfated proteoglycans (Patel et al., 2001). These observations emphasize the importance of the microenvironment when studying tumor cell behavior, particularly with regards to chemokine signaling.

Paracrine effects: CCR7-mediated tumor cell chemotaxis towards LECs

We first used our co-culture model (Fig. 1B) to investigate tumor cell chemotaxis through a 3D matrix towards LECs under static conditions. For baseline migration (without LECs), the blocking antibodies did not affect migration/invasion in all cases (Fig. 4A-D). This suggested that CCR7 signaling was not important for random migration through a 3D matrix.

When LECs were present, the benign MCF10A mammary epithelial cells migrated preferentially towards LECs, but in a CCR7-independent manner since a cocktail of neutralizing antibodies against CCR7 and CCL21 did not inhibit chemotaxis (Fig. 4A-D). MCF7 cells, which displayed higher CCR7 levels than did MCF10A, responded in a similar manner, although CCR7/CCL21 blocking had a slight (but not statistically significant) affect on reducing chemotaxis. However, in the two highly invasive cell lines, ZR-75-1 and MDA-MB-435S, chemotaxis towards LECs was significantly higher than that demonstrated in the other cell lines (Fig. 4E), and was strongly CCR7 dependent, since CCR7/CCL21 neutralization abolished this chemotactic response. These results demonstrate that LECs chemoattract tumor cells through a 3D matrix via CCR7 signaling, and CCR7-expressing tumor cells are more chemoattracted to LECs than non-CCR7 expressing cells, at least for the mammary carcinoma cell lines tested here.

Autologous chemotaxis of tumor cells by interstitial flow

To individually investigate the effects of interstitial flow on autologous chemotaxis of tumor cells, we introduced very slow flow (0.2 μm/s, which is within measured *in vivo* values (Chary and Jain, 1989; Dafni et al., 2002)) through the tumor cell-seeded Matrigel in the absence of LECs. Strikingly, we found that this low flow drove the same chemotactic response of tumor cells as did the LECs (Fig. 5). In the MCF10A cells, which expressed the lowest amount of

CCR7, flow enhanced migration to a small but significant degree, but this enhancement was not affected by blocking CCR7 signaling (Fig. 5A). In contrast, the three tumor cell lines displayed more substantial invasiveness in the flow direction that was CCR7 dependent (Figs. 5B-D). Furthermore, their response was loosely correlated with their CCR7 receptor and ligand expression: ZR-75-1 and MDA cells displayed the strongest “autologous chemotaxis” response to flow. Thus, the flow-enhanced migration of the 3 different carcinoma cell lines was indeed a chemotactic response (summarized in Fig. 5E), yet no exogenous chemokine had been applied (and in fact the experiments were performed in serum-free basal media), nor was any other cell type present to direct signaling. Because only tumor cells were present, the ligands that induced CCR7 signaling necessarily came from the tumor cells themselves. Our results clearly demonstrate that autologous chemotaxis up CCR7 ligand gradients occurred in these tumor cells under interstitial flow.

Interestingly, the amount of migration in response to flow when CCR7 signaling was blocked was roughly equal in all four cell lines, despite their varying responses to flow (Fig. 5F). This suggested that flow had an additional effect that was CCR7-independent. It is probable that this increase was solely a consequence of directed proteolysis, as the pan-MMP inhibitor GM6001 abolished all flow-enhanced migration (data not shown).

To visualize cell polarization under flow as a direct indicator of autologous chemotaxis, we created a high-efficiency stable transduction of the PHAKT-eGFP transgene in ZR-75-1 cells using a lentiviral vector. This enabled us to follow distribution and localization of the pleckstrin homology domain of the signaling molecule AKT, an early signaling event indicating polarization and alluding to cell movement (Servant et al., 2000). PHAKT, normally localized in the cytoplasm, becomes recruited to the plasma membrane as part of a receptor signaling

complex when, following cellular stimulation, actin cytoskeleton reorganization is required (e.g. during chemotaxis). In static 3D conditions, we found PHAKT-eGFP localization to be weak and randomly directed (Fig. 6A). However, under IF, localization was visibly enhanced and most cells were polarized in the general direction of flow (Fig. 6B), indicating that the flow-induced signals were priming the cytoskeletal machinery for a migration response. As a positive control, we saw a similar biased PHAKT localization in the direction of an imposed CCL21 gradient under static conditions (Fig. 6C, with a cell in 2D exposed to the same CCL21 gradient shown in Fig. 6D as a comparison).

To quantify this effect, each cell was scored (Fig. 6E) and classified as (*i*) not polarized, (*ii*) polarized in the direction of flow (region I, 0-60^{o}), (*iii*) polarized orthogonal to the direction of flow (region II, from 60-120^{o}), or (*iv*) polarized against the direction of flow (region III, 120-180^{o}). In all cases – static, flow, and static with an imposed exogenous CCL21 gradient - more than half of all cells did not show any polarization. In those cells that did polarize, there was no directional bias seen in static conditions, but those cells under flow displayed a four-fold increase in directional bias towards flow (Fig. 6F). This mimicked the response seen in cells exposed to a static exogenous CCL21 gradient, which also showed a four-fold increase in directional bias towards the direction of increasing concentration. Hence under static conditions there is no biasing factor and cells polarize randomly, whereas in contrast, after exposure to biasing factors such as slow interstitial flow or chemoattractive gradients, intracellular signals can propel the cell to polarize at the leading edge prior to actin cytoskeletal reorganization and directional migration towards the stimuli. Therefore, slow interstitial flow induced a similar effect on cell polarization as did an exogenous CCL21 protein gradient of 3.5 µg/ml/mm. This further supported the notion

that interstitial flow could indeed induce an autologous chemotactic response in cells that express both the CCR7 receptor and ligand.

Combined effects of flow and LECs leads to amplified response

Finally, we examined the combined response of tumor cells to LECs and interstitial flow (Fig. 1A). We performed these experiments on the MDA-MB-435S cells as they exhibited the strongest chemotactic response in both individual cases. As expected, the two effects combined to drive even stronger chemotaxis in the direction of LECs and interstitial flow than either factor alone (Fig. 7A). In the combined effects, the conditions “control static” and “control block” represented LECs alone, with and without blocking antibodies, as before. Combined, flow-enhanced migration of tumor cells towards LECs was roughly three times that of their migration towards either cue alone. When CCR7 signaling was blocked, the percent migration was not significantly different than either that seen with flow alone under blocking, or with LECs alone plus blocking, indicating that the combined effect was also CCR7 mediated.

Computational modeling of the tumor-lymphatic microenvironment

To explain the autologous chemotactic effects observed, we hypothesized that interstitial flow could skew the release of matrix-binding CCL21 and CCL19 by the tumor cell, and, together with slight biasing of cell-released proteases that liberate the chemokine from the matrix, create pericellular gradients of autocrine CCR7 ligands. If transcellular CCL21/19 gradients form, the cell would presumably respond by migrating in the direction of the higher concentration. This was based on recent findings that low levels of flow could synergize with matrix-bound vascular endothelial growth factor (VEGF) to drive capillary morphogenesis *in*

vitro (Helm et al., 2005), and on recent computational modeling that described how such gradients might be formed (Fleury et al., 2006). It is important to note that under such conditions, diffusion still strongly dominates the overall transport problem – the Peclet number, which describes the relative contribution of convection compared to diffusion in the overall transport, is only 0.02 – but convective transport despite it being so small compared to diffusion, is necessary to facilitate the transcellular chemokine gradient.

We modeled the specific case of CCR7 ligands (CCL21/19) secreted by a cell into the pericellular matrix under 0.2 μm/s flow. First, CCL21/19 was assumed to be secreted uniformly from a 20-μm cell at constant flux and transported away from the cell by diffusion and convection, and was also subject to matrix binding according to its local concentration and its k_{on} and k_{off}. The same cell was also considered to secrete matrix degrading enzymes (MMPs, sulfatases, etc) that were capable of further liberating ECM-bound CCL21/19, so that the final soluble CCL21/19 profile was a combination of cell-secreted and ECM-released ligands, and only this soluble fraction of ligands was assumed to signal the cell receptor. This differs from the cases that we have presented previously, where ligand was initially present uniformly bound to the matrix (Helm et al., 2005), or where ligand was secreted in a pro-form and only active upon protease cleavage (Fleury et al., 2006). Finally, we modeled all experimental cases, considering individually LEC-induced paracrine signaling as well as autologous signaling, both under conditions of static vs. flow, and with and without CCR7 blocking.

The computational results were qualitatively consistent with our experimental results. First, paracrine effects of LEC-secreted CCL21 (under static conditions) induced a small (1.0%) transcellular ligand gradient across the tumor cell surface (Fig. 7B). Due to the experimental and modeled geometry, CCL21 diffusion from the LEC monolayer was one-dimensional, and

therefore the LEC-induced gradient around a tumor cell was relatively independent of tumor cell to LEC distance within the 500 μm thick matrix; however, *in vivo*, we would expect this gradient to have a much stronger dependence on the distance between the tumor cell and lymphatic vessel because (1) the geometry is such that CCL21 concentration would diminish much more drastically as a function of distance, (2) the total flux of CCL21 coming from the lymphatic would be much lower *in vivo* since the lymphatic endothelium of an intact capillary contains a much lower density of lymphatic endothelial cells than a cultured monolayer: a single LEC is extremely elongated and thinly stretched *in vivo*.

We then modeled autocrine effects and saw that slow interstitial flow can bias both CCL21/19 transcellular gradient and also cell-secreted enzymes (Fig. 7B) in the direction of flow, and in the absence of LECs. The biased distribution of enzyme would subsequently impact the liberation of bound chemokine downstream generating a soluble chemokine gradient. These data correspond well with the results of the *in vitro* migration assay (Figs. 7A and 7D). Specifically, we found that the calculated transcellular gradient for a tumor cell under flow (1.2%) was similar to that under static conditions but in the presence of LECs (1.0%), which was consistent with the experimental data where these two conditions had each induced similar migration responses (1.3% and 1.1% flow alone and LECs alone respectively).

When both effects were combined, the transcellular gradient was increased approximately 3-fold to 3.6%, and this was strikingly consistent with the experimental results showing that the percentage of transmigrated cells was also roughly tripled compared to either LECs alone or flow alone. While we have hypothesized that migration is principally driven by biased CCL21/19 gradients, a secondary mechanism may also be present: soluble enzymes secreted by tumor cells are also subject to the biasing effects of interstitial flow, and enzyme gradients could lead to

slightly increased migration in the direction of flow due to directed proteolysis. While CCR7 blocking should abolish the hypothesized chemotactic mechanism, it would not affect directed proteolysis (Fig 7B). Consistent with this notion, *in vitro* migration experiments show that while CCR7 blocking inhibits flow-enhanced migration, there still remain some residual enhancement of migration (although not statistically significant in any cell type) compared to that in static controls (Fig. 7A).

Thus, our experimental results clearly demonstrate that flow-enhanced migration is due to CCR7-mediated chemokine signaling, and our computational model offers a mechanistic explanation of autologous chemotaxis.

Discussion

This study highlights the importance and relevance of the biophysical microenvironment to lymphatic metastasis and introduces a new mechanism that we term autologous chemotaxis whereby autocrine chemokine secretion can direct tumor cells to chemotact in the direction of flow, i.e., towards draining lymphatics. It provides mechanistic insight into why CCR7 expression is increasingly found to correlate with lymph node metastasis in human cancers (Cabioglu et al., 2005; Gunther et al., 2005; Heresi et al., 2005; Takeuchi et al., 2004; Wang et al., 2005; Wiley et al., 2001), and introduces data showing that tumor invasiveness may also be correlated with autocrine secretion of CCR7 ligands. Furthermore, when the tumor cell comes in close proximity to a lymphatic, which can also secrete CCL21, the tumor-derived CCL21/19 gradient can add to the lymphatic-secreted CCL21 to further augment the chemotactic response. This is consistent with the increase we saw in tumor cell migration when LECs were present, both in static and flow conditions, compared to when LECs were not present. Interestingly, while interstitial flow decreases the transport of CCL21 secreted by the lymphatics, it actually *increases*

the transcellular gradient across a nearby tumor cell (within its broadcast distance), since the concentration gradient becomes steeper. This is important since chemotacting cells respond to a concentration difference rather than an absolute amount (Zigmond 1977).

Because interstitial flow is always directed from the tumor toward the lymphatic, and because chemokine signaling appears to play a critical role in lymphatic homing of tumor cells, an experimental model system to study tumor-lymphatic interactions should include both appropriate levels of interstitial flow and allow for natural chemokine signaling to occur. To date, experimental model systems of tumor-lymphatic interactions have been limited to human tumor xenografts in mice, where relative migration is difficult to assess, and where chemokine signaling can be altered due to a compromised immune system and potential incompatibilities between some rodent and human cytokines. Standard *in vitro* chemotaxis assays typically do not include biophysical factors, like ECM and IF, which could strongly affect the transport and distribution of secreted chemokines and thus relevant cell-cell signaling events. Tissue engineered 3D models have advantages over both *in vivo* and traditional *in vitro* models for examining interactions between human cells in an environment that recapitulates some of the biophysical features of the natural *in vivo* situation (Griffith and Swartz, 2006).

Using a unique 3D co-culture model we demonstrate how the biophysical factors of the tumor-lymphatic microenvironment might favor tumor cell migration towards lymphatics. We saw that tumor cells secrete CCL21 and CCL19, and also that they do so to a much higher degree when maintained within a 3D matrix than when cultured in 2D. Furthermore, these cells are responsive to CCR7 ligand and can chemotact both up an imposed CCL21 gradient and towards LECs in a CCR7-dependent manner. Strikingly, physiological levels of interstitial flow significantly enhanced tumor migration in the direction of flow, with and without LECs. These

responses could be reversed by blocking CCR7 signaling, clearly illustrating that flow-enhanced migration is a phenomenon of CCR7-dependent chemotaxis. A computational simulation of CCL21/19 transport under this flow estimated the transcellular CCL21/19 gradient to be 1.2% without LECs and 3.6% with LECs (in the direction of flow). Although the limits for tumor cell response to CCL21/19 gradient detection are not known, it has been shown that neutrophils can directionally sense as little as 1% differences in transcellular concentration of the chemoattractant N-formylmethionyl peptides (Zigmond, 1977), and small morphogen gradients act as essential positional cues for cells in many developing tissues (Ashe and Briscoe, 2006; Yucel and Small, 2006; Gurdon and Bourillot, 2001). Furthermore, we demonstrated, using the PHAKT-eGFP cell polarization marker, that such imposed biophysical cues alone were capable of initiating the cellular signaling events needed for actin reorganization and directional migration. Thus, it is highly probable that small transcellular chemokine gradients formed by flow are responsible for stimulating polarization and subsequent chemotaxis of tumor cells in the direction of flow that we observed.

This mechanism is relevant to other cell chemotaxis events in an environment with interstitial flow. For example, we found earlier that interstitial flow acted synergistically with matrix-bound VEGF to drive enhanced and directed endothelial cell organization into capillaries *in vitro* (Helm et al., 2005). Our findings also provide an alternative mechanism to tumor lymphangiogenesis that may explain why VEGF-C-secreting tumor cells are more highly metastatic (Wong et al., 2005). Any chemokine-secreting tumor cell could use autologous chemotaxis to augment homing to lymphatics, provided they express the receptor, but in addition, VEGF-C secretion could help facilitate their entry into lymphatics by rendering the draining lymphatic vessels hyperplastic (Jeltsch et al., 1997; Goldman et al., 2005) and therefore potentially more susceptible to invasion.

In conclusion, using a physiologically relevant tissue culture model we have demonstrated the importance of the tumor-ECM-lymphatic microenvironment for lymphatic metastasis and identified a new mechanism for tumor cell homing to lymphatics that is consistent with human cancer data correlating CCR7 expression with lymph node metastasis. In addition, this is the first demonstration that (1) tumor cells are chemotactically attracted to LECs via CCR7 signaling, (2) physiological levels of interstitial flow enhances tumor cell migration, and (3) tumor cells can chemotact in the flow direction via autologous chemokine signaling. These results help elucidate fundamental mechanisms of tumor cell invasion of lymphatics and may be relevant to understanding how lymphocytes also home to lymphatics.

Methods

Antibodies, flow cytometry, and immunofluorescence

Neutralizing antibodies against human CCL21 (AF366) and CCR7 (MAB197) were purchased from R&D Systems (Minneapolis, MN) and used at 4µg/ml and 5µg/ml respectively. Antibodies against human podoplanin (gp36; 10µg/mL, Cell Sciences, Inc., Canton, MA), CD31 (10µg/mL, BD Pharmingen, San Diego, CA), LYVE-1 (15µg/mL, RELIATech, Braunschweig, Germany), and Prox1 (5µg/mL, RELIATech) were used along with mouse IgG as a control (10µg/mL, Sigma). AlexaFluor 488-labeled IgGs (Molecular Probes, Carlsbad, CA) were used for detection, and DAPI (Vector Laboratories) for counterstaining nuclei in immunofluorescence. Flow cytometry was performed using a FACScan (Becton Dickinson) and analyzed with FlowJo software (Tree Star, Inc., Ashland, OR).

Cell Culture

MCF10A, MCF7, ZR-75-1, and MDA-MB-435S cells were all purchased from ATCC/LGC Promochem (Middlesex, UK) and maintained in 1:1 DMEM:F12 Hams (supplemented with 0.01mg/ml bovine insulin, 0.5µg/ml hydrocortisone, 20ng/ml EGF, 5% FBS and 1% penicillin-streptomycin), alpha-MEM (supplemented with 2mM L-glutamine, 1mM sodium pyruvate, 0.01mg/ml bovine insulin, 10% FBS and 1% penicillin-streptomycin), RPMI 1640 (supplemented with 2.5g/l D-glucose, 1mM sodium pyruvate, 10mM HEPES, 10% FBS and 1% penicillin-streptomycin), and DMEM with 10% FBS, respectively. Human dermal LECs were isolated from neonatal foreskin and cultured as previously described (Podgrabinska et al., 2002). Human dermal fibroblasts, used for negative controls for LEC marker expression (data not shown), were obtained from Cambrex and cultured in DMEM with 10% FBS.

Static migration assay

Experiments were performed with 12 mm, 8µm pore cell culture inserts (Millipore, Billerica, MA) in a modified Boyden chamber assay. For chemotactic gradient studies, 50,000 tumor cells were seeded in 150µl matrigel (4.65mg/ml, BD Biosciences; ST Jose, CA), which created a gel of 1mm thickness. The medium in the top chamber was basal medium, while that in the bottom was basal medium either alone, with 350ng/ml CCL21 protein, or with both CCL21 protein and a cocktail of anti-CCR7 and anti-CCL21 blocking antibodies (in the latter case, antibodies were also included in the top chamber). After 15h in a 37ºC / 5% CO_2 incubator, matrigel containing non-migrated cells was removed and the inserts were fixed in chilled methanol for 15min, 4ºC. The membrane was removed and mounted with Vectashield containing DAPI (Vector), and the number of migrated cells was counted to allow calculation of normalized migration.

Co-culture migration assay

For assessing chemotaxis of tumor cells towards LECs a co-culture assay, modified from the above set-up was used. LECs were seeded onto the previously collagen coated underside of the chamber at 100,000 per well and cultured for 3 days into a monolayer. The migration assay was then prepared as described above but modified to incorporate 50,000 tumor cells seeded in 50µl matrigel. This assay was performed with MDA-MB-435S cells.

Migration under flow

The above setup was modified to examine the effects of physiological flow on tumor cell migration, either with or without LECs on the underside of the chamber as described. After the matrigel was cast and allowed to set (1h), a pressure head of 1cm water was established that led to an average velocity of 0.2 µm/s through the cell/gel compartment. To measure the flow rate, we performed separate experiments in which we weighed the effluent fluid at many time points (with care to avoid evaporation by doing the experiments in a 37°C, 100% humid environment and keeping the effluent collecting tube closed off), and also measured the movement of a bubble in a thin capillary tube downstream. Furthermore, we did separate hydraulic permeability measurements of the gels, by comparing pressure-flow relationships under different gel thicknesses, to verify our flow calculations. These flow values were then verified with permeability calculations. Migration in the presence of basal media, either alone or with anti-CCR7 and anti-CCL21 blocking antibodies, was assessed for all cell lines. Each condition was performed with matching static controls.

Western blot analysis

Cell lysates from each tumor cell line and LECs were analyzed by Western blot using 10µg/ml goat anti-CCR7 (Abcam), HRP-conjugated rabbit anti-goat IgG (BioRad), and a Western Pico ECL substrate kit (Pierce, Rockford, IL). Samples loads were normalized to cell number in three separate experiments.

ELISA

CCL19 and CCL21 protein secretion was quantified from cells maintained in both 2D and 3D culture conditions in basal media. For 2D samples, conditioned media was collected after 24 hours of culture. 3D samples were produced when cells were suspended within 300µl of Growth Factor Reduced Matrigel matrix in basal media at a density of 450,000 cells per well of a 24 well plate. After culture, three compartments were analyzed by ELISA: medium, matrix protein (by digestion with Cell Recovery Solution (BD Biosciences; ST Jose, CA)), and cells (by lysis using standard RIPA buffer protocols (Sigma)). CCL19 Duoset and CCL19 Quantikine ELISA kits (both R&D) were used according to manufacturers' guidelines. 100µl conditioned media from each cell type after 24 hours in culture was used followed by cell harvest and counting to determine amount of chemokine secreted (pg) per 1000 cells per 24 h.

Computation of Extracellular CCL21 Distribution

Pericellular CCL21 gradients were computed using a 3D model according to the governing equation:

$$\frac{dC_i}{dt} + v\nabla C_i = D_i\nabla^2 C_i + R_i$$

where C_i is concentration of species i, t is time, v is velocity, D_i is the diffusion coefficient, and R_i is the rate of reaction (disappearance due to matrix binding or appearance due to unbinding or proteolytic release from the matrix). The cell was modeled as a 20 μm diameter sphere embedded in a 500 μm thick porous ECM (Matrigel) with 3 mm of medium atop the matrix. The Brinkman equation was used to calculate the velocity profile through the porous ECM around the cell using a value for permeability $K = 10^{-12}$ cm^2 (calculated from our experimental data using Darcy's law) and average v (far-field velocity) = 0.2 μm/s. Three species i were modeled: cell-released soluble enzyme, cell-released CCL21/19 (which was considered as one chemokine ligand species), and matrix-bound CCL21/19. Boundary conditions were considered to be constant cell flux for both the protease and cell-secreted CCL21/19, and a zero flux inlet boundary condition for these two species. The diffusion coefficients in Matrigel were assumed to be approximately 70% that of the calculated value in free liquid using the relationship of $D_o = 3600(MW)^{(-0.34)}$, where D_o is the diffusion coefficient in free solution at 23°C and MW is the protein molecular weight (Berk et al, 1993), and then adjusted to that at 37°C using the Stokes-Einstein relationship. The diffusion coefficients calculated as such were 140 μm^2/s for CCL21/19 and 80 μm^2/s for cell-released enzyme (which represented any protease that could liberate matrix-bound chemokine). The modeled species were subjected to the following binding and release kinetics:

$$CCL + HS \underset{koff}{\overset{kon}{\leftrightarrow}} HS - CCL$$

$$HS - CCL + E \xrightarrow{krel} CCL + S' + E$$

where *CCL* = CCL21/19, *HS* and *HS'* = heparin sulfate binding sites and denatured binding sites, respectively, *HS-CCL* = matrix-bound CCL21/19, *E* = enzyme (secreted protease), and k_{on}, k_{off} and k_{rel} are rate constants for the reactions shown.

The corresponding rate equations were:

$$R_{CCL} = -k_{on}C_{CCL}C_{HS} + k_{off}C_{HS-CCL} + k_{rel}C_{HS-CCL}C_{enz}$$

$$R_{HS-CCL} = k_{on}C_{CCL}C_{HS} - k_{off}C_{HS-CCL} - k_{rel}C_{HS-CCL}C_{enz} = -R_{CCL}$$

where *R* refers to the overall rate of production and *C* refers to the concentration of each of the components defined above.

The equilibrium binding coefficient K_d was defined as:

$$K_d = \frac{C_{CCL}C_{HS}}{C_B} = \frac{k_{off}}{k_{on}}$$

Thus the rate equation was simplified to:

$$R_{HS-CCL} = k_{on}C_{CCL}C_{HS} - K_d k_{on}C_{HS-CCL} - k_{rel}C_{HS-CCL}C_{enz}$$

In our case, C_{HS} was considered to be much larger than C_{CCL} based on the calculated number of binding sites in the Matrigel relative to the total CCR7 ligand concentration as determined by ELISA, and therefore was treated as a constant; K_d has been measured for CCL21 binding to heparin sulfate proteoglycans as 5.5 nM (Uchimura et al, 2006), and k_{on} was estimated as 10^{-3} nM^{-1} s^{-1} based on kinetic data for other heparin binding compounds (Nugent and Edelman, 1992). The concentration of binding sites in Growth Factor Reduced Matrigel was calculated assuming 2% proteoglycan (perlecan) content (based on data from the manufacturer) and 12 binding sites per molecule of perlecan in recognition of the multiple proteoglycan chains attached to each perlecan core protein. Parametric variation of k_{rel} revealed that while absolute concentrations

were somewhat sensitive to this parameter, the percent transcellular gradients were not significantly affected.

Cell secretion of CCL21 and CCL19 was determined experimentally (Fig. 3). Mass balances for free ligand, bound ligand, and protease (enzyme) were solved simultaneously in a transient analysis to estimate the gradients that would be established after 50,000 seconds, matching the experimental time frame. The calculations were performed using COMSOL Multiphysics modeling software (Berne, Switzerland) on a personal computer.

PHAKT-eGFP polarization assay

The fluorescent probe used to determine spatial distribution of intermediate intracellular signals between activation of chemotactic receptors and actin polymerization, the PHAKT-eGFP construct (Servant et al., 2000), was a kind gift from Tamas Balla. A cassette containing the PHAKT-eGFP, a *EcoRI-HincII* fragment, was blunt-end ligated into the lentivirus backbone pRRLsincPPT-hPGK-mcs-WPRE (a kind gift from Didier Trono) and expanded in competent E.coli. Clone DNAs from antibiotic-resistant colonies were purified and analyzed for the correct recombination event. Lentiviral vectors were produced via transfection of HEK293T cells with the PHAKT-eGFP transfer construct, pCMVR8.74 packaging plasmid and pMD2.G envelope plasmid in the ratio 3:2:1. Media were collected after 24 and 36 hours and virus was concentrated by ultracentrifugation in 20% saccarose solution. ZR-75-1 cells were infected with the lentivirus in 24 well plates, and checked for stable expression of PHAKT-eGFP.

PHAKT-eGFP-ZR-75-1 cells were seeded at 10^6 cells/ml within a matrix (3:1 collagen:Matrigel) and placed within a radial flow chamber as described (Ng et al., 2005). Slow IF, via a constant pressure head of 1cm H_2O (leading to an average flow velocity of ~0.2 μm/s

near the outer edge of the chamber, where images were taken) was applied to the system for 7 hours (maintained at 37ºC/5% CO_2 on the microscope stage), during which time live cells were visualized on a Zeiss fluorescence microscope (Axiovert 200M).

For cells exposed to an exogenous CCL21 gradient in 2D or 3D, PHAKT-eGFP-ZR-75-1 cells were seeded into an IBIDI µVI culture slide (Ibidi, Munich, Germany) either in basal medium or in Matrigel and allowed to establish overnight. 350 ng/ml CCL21 and basal medium to the other, with a 1cm distance separating the two. Cells were maintained in this gradient for 20 minutes or 6 hours (2D and 3D respectively) and then cells within a few hundred microns of the CCL21 depot were visualized with a Zeiss fluorescence microscope.

Statistical analyses

To test for statistical significance between experimental groups, Kruskal-Wallis and Mann-Whitney U tests were performed. Statistical significance was assumed where $p<0.05$.

Acknowledgements

The authors thank Olga Sazonova, Thomas Le, Didier Foretay, Veronique Borel, Alexander Shoushtari, and Ulrike Haessler for technical assistance; Mihaela Skobe and Simona Podgrabinska for help with LEC isolation; Isabelle Barde and Didier Trono for assistance with lentiviral production; and Tamas Balla for the generous gift of the PHAKT-eGFP construct. This work was funded by the U.S. D.o.D. (BC046063), the N.I.H. (RO1 HL075217-01), and the Swiss National Science Foundation (107602).

References

Achen, M. G., McColl, B. K., and Stacker, S. A. (2005). Focus on lymphangiogenesis in tumor metastasis. Cancer Cell *7*, 121-127.

Arya, M., Patel, H. R., McGurk, C., Tatoud, R., Klocker, H., Masters, J., and Williamson, M. (2004). The importance of the CXCL12-CXCR4 chemokine ligand-receptor interaction in prostate cancer metastasis. J Exp Ther Oncol *4*, 291-303.

Ashe, H. L., and Briscoe, J. (2006). The interpretation of morphogen gradients. Development *133*, 385-394.

Berk, D.A., Yuan, F., Leunig, M., and Jain, R.K. (1993). Fluorescence photobleaching with spatial Fourier analysis: measurement of diffusion in light-scattering media. Biophys J *65*, 2428-2436.

Cabioglu, N., Yazici, M. S., Arun, B., Broglio, K. R., Hortobagyi, G. N., Price, J. E., and Sahin, A. (2005). CCR7 and CXCR4 as novel biomarkers predicting axillary lymph node metastasis in T1 breast cancer. Clin Cancer Res *11*, 5686-5693.

Cailleau, R., Olive, M., and Cruciger, Q. V. (1978). Long-term human breast carcinoma cell lines of metastatic origin: preliminary characterization. In Vitro *14*, 911-915.

Carmeliet, P. (2003). Angiogenesis in health and disease. Nature Med *9*, 653-660.

Chambers, A. F., Groom, A. C., and MacDonald, I. C. (2002). Dissemination and growth of cancer cells in metastatic sites. Nature Rev Cancer *2*, 563-572.

Chary, S. R., and Jain, R. K. (1989). Direct measurement of interstitial convection and diffusion of albumin in normal and neoplastic tissues by fluorescence photobleaching. Proc Natl Acad Sci U S A *86*, 5385-5389.

Clarijs, R., Schalkwijk, L., Ruiter, D. J., and de Waal, R. M. (2001). Lack of lymphangiogenesis despite coexpression of VEGF-C and its receptor Flt-4 in uveal melanoma. Invest Ophthalmol Vis Sci *42*, 1422-1428.

Dafni, H., Israely, T., Bhujwalla, Z. M., Benjamin, L. E., and Neeman, M. (2002). Overexpression of vascular endothelial growth factor 165 drives peritumor interstitial convection and induces lymphatic drain: magnetic resonance imaging, confocal microscopy, and histological tracking of triple-labeled albumin. Cancer Res *62*, 6731-6739.

Darash-Yahana, M., Pikarsky, E., Abramovitch, R., Zeira, E., Pal, B., Karplus, R., Beider, K., Avniel, S., Kasem, S., Galun, E., and Peled, A. (2004). Role of high expression levels of CXCR4 in tumor growth, vascularization, and metastasis. FASEB J *18*, 1240-1242.

Debes, G. F., Arnold, C. N., Young, A. J., Krautwald, S., Lipp, M., Hay, J. B., and Butcher, E. C. (2005). Chemokine receptor CCR7 required for T lymphocyte exit from peripheral tissues. Nature Immunol *6*, 889-894.

Ding, Y., Shimada, Y., Maeda, M., Kawabe, A., Kaganoi, J., Komoto, I., Hashimoto, Y., Miyake, M., Hashida, H., and Imamura, M. (2003). Association of CC chemokine receptor 7 with lymph node metastasis of esophageal squamous cell carcinoma. Clin Cancer Res *9*, 3406-3412.

Engel, L. W., Young, N. A., Tralka, T. S., Lippman, M. E., O'Brien, S. J., and Joyce, M. J. (1978). Establishment and characterization of three new continuous cell lines derived from human breast carcinomas. Cancer Res *38*, 3352-3364.

Fleury, M. E., Boardman, K. C., and Swartz, M. A. (2006). Autologous Morphogen Gradients by Subtle Interstitial Flow and Matrix Interactions. Biophys J *91*, 113-121.

Forster, R., Schubel, A., Breitfeld, D., Kremmer, E., Renner-Muller, I., Wolf, E., and Lipp, M. (1999). CCR7 coordinates the primary immune response by establishing functional microenvironments in secondary lymphoid organs. Cell *99*, 23-33.

Goldman, J., Le, T. X., Skobe, M., and Swartz, M. A. (2005). Overexpression of VEGF-C causes transient lymphatic hyperplasia but not increased lymphangiogenesis in regenerating skin. Circ Res *96*, 1193-1199.

Griffith, L., and Swartz, M. (2006). Capturing complex 3D tissue physiology *in vitro*. Nature Rev Mol Cell Biol *7*, 211-224.

Gunn, M. D., Tangemann, K., Tam, C., Cyster, J. G., Rosen, S. D., and Williams, L. T. (1998). A chemokine expressed in lymphoid high endothelial venules promotes the adhesion and chemotaxis of naive T lymphocytes. Proc Natl Acad Sci U S A *95*, 258-263.

Gunther, K., Leier, J., Henning, G., Dimmler, A., Weissbach, R., Hohenberger, W., and Forster, R. (2005). Prediction of lymph node metastasis in colorectal carcinoma by expressionof chemokine receptor CCR7. Int J Cancer *116*, 726-733.

Gurdon, J.B., and Bourillot, P.Y. (2001). Morphogen gradient interpretation. Nature *413*, 797-803.

Handel, T.M., Johnson, Z., Crown, S.E., Lau, E.K., Sweeney, M., and Proudfoot, A.E. (2005). Regulation of protein function by glycosaminoglycans - as exemplified by chemokines. Ann Rev Biochem *74*, 385-410.

He, Y., Rajantie, I., Pajusola, K., Jeltsch, M., Holopainen, T., Yla-Herttuala, S., Harding, T., Jooss, K., Takahashi, T., and Alitalo, K. (2005). Vascular endothelial cell growth factor receptor 3-mediated activation of lymphatic endothelium is crucial for tumor cell entry and spread via lymphatic vessels. Cancer Res *65*, 4739-4746.

Helm, C. L., Fleury, M. E., Zisch, A. H., Boschetti, F., and Swartz, M. A. (2005). Synergy between interstitial flow and VEGF directs capillary morphogenesis in vitro through a gradient amplification mechanism. Proc Natl Acad Sci U S A *102*, 15779-15784.

Heresi, G. A., Wang, J., Taichman, R., Chirinos, J. A., Regalado, J. J., Lichtstein, D. M., and Rosenblatt, J. D. (2005). Expression of the chemokine receptor CCR7 in prostate cancer presenting with generalized lymphadenopathy: report of a case, review of the literature, and analysis of chemokine receptor expression. Urol Oncol *23*, 261-267.

Jain, R. K. (2003). Molecular regulation of vessel maturation. Nature Med *9*, 685-693.

Jain, R. K. (2005). Normalization of tumor vasculature: an emerging concept in antiangiogenic therapy. Science *307*, 58-62.

Jeltsch, M., Kaipainen, A., Joukov, V., Meng, X., Lakso, M., Rauvala, H., Swartz, M., Fukumura, D., Jain, R. K., and Alitalo, K. (1997). Hyperplasia of lymphatic vessels in VEGF-C transgenic mice. Science *276*, 1423-1425.

Kimsey, T. F., Campbell, A. S., Albo, D., Wilson, M., and Wang, T. N. (2004). Co-localization of macrophage inflammatory protein-3alpha (Mip-3alpha) and its receptor, CCR6, promotes pancreatic cancer cell invasion. Cancer J *10*, 374-380.

Mandriota, S. J., Jussila, L., Jeltsch, M., Compagni, A., Baetens, D., Prevo, R., Banerji, S., Huarte, J., Montesano, R., Jackson, D. G., *et al.* (2001). Vascular endothelial growth factor-C-mediated lymphangiogenesis promotes tumour metastasis. EMBO J *20*, 672-682.

Mashino, K., Sadanaga, N., Yamaguchi, H., Tanaka, F., Ohta, M., Shibuta, K., Inoue, H., and Mori, M. (2002). Expression of chemokine receptor CCR7 is associated with lymph node metastasis of gastric carcinoma. Cancer Res *62*, 2937-2941.

Muller, A., Homey, B., Soto, H., Ge, N., Catron, D., Buchanan, M. E., McClanahan, T., Murphy, E., Yuan, W., Wagner, S. N., *et al.* (2001). Involvement of chemokine receptors in breast cancer metastasis. Nature *410*, 50-56.

Murakami, T., Cardones, A. R., and Hwang, S. T. (2004). Chemokine receptors and melanoma metastasis. J Dermatol Sci *36*, 71-78.

Nathanson, S. D. (2003). Insights into the mechanisms of lymph node metastasis. Cancer *98*, 413-423.

Ng, C. P., Hinz, B., and Swartz, M. A. (2005). Interstitial fluid flow induces myofibroblast differentiation and collagen alignment in vitro. J Cell Sci *118*, 4731-4739.

Nugent, M.A., and Edelman, E.R. (1992). Kinetics Of Basic Fibroblast Growth-Factor Binding To Its Receptor And Heparan-Sulfate Proteoglycan - A Mechanism For Cooperativity. Biochem *31*, 8876-8883.

Ohl, L., Mohaupt, M., Czeloth, N., Hintzen, G., Kiafard, Z., Zwirner, J., Blankenstein, T., Henning, G., and Forster, R. (2004). CCR7 governs skin dendritic cell migration under inflammatory and steady-state conditions. Immunity *21*, 279-288.

Patel, D. D., Koopmann, W., Imai, T., Whichard, L. P., Yoshie, O., and Krangel, M. S. (2001). Chemokines have diverse abilities to form solid phase gradients. Clin Immunol *99*, 43-52.

Podgrabinska, S., Braun, P., Velasco, P., Kloos, B., Pepper, M. S., and Skobe, M. (2002). Molecular characterization of lymphatic endothelial cells. Proc Natl Acad Sci U S A *99*, 16069-16074.

Randolph, G. J., Angeli, V., and Swartz, M. A. (2005). Dendritic-cell trafficking to lymph nodes through lymphatic vessels. Nature Rev Immunol *5*, 617-628.

Servant, G., Weiner, O. D., Herzmark, P., Balla, T., Sedat, J. W., and Bourne, H. R. (2000). Polarization of chemoattractant receptor signaling during neutrophil chemotaxis. Science *287*, 1037-1040.

Sipos, B., Kojima, M., Tiemann, K., Klapper, W., Kruse, M. L., Kalthoff, H., Schniewind, B., Tepel, J., Weich, H., Kerjaschki, D., and Kloppel, G. (2005). Lymphatic spread of ductal pancreatic adenocarcinoma is independent of lymphangiogenesis. J Pathol *207*, 301-312.

Skobe, M., Hawighorst, T., Jackson, D. G., Prevo, R., Janes, L., Velasco, P., Riccardi, L., Alitalo, K., Claffey, K., and Detmar, M. (2001). Induction of tumor lymphangiogenesis by VEGF-C promotes breast cancer metastasis. Nature Med *7*, 192-198.

Soule, H. D., Vazguez, J., Long, A., Albert, S., and Brennan, M. (1973)A human cell line from a pleural effusion derived from a breast carcinoma. J. Natl. Cancer Inst *51*, 1409-1416.

Soule, H. D., Maloney, T. M., Wolman, S. R., Peterson, W. D., Jr., Brenz, R., McGrath, C. M., Russo, J., Pauley, R. J., Jones, R. F., and Brooks, S. C. (1990). Isolation and characterization of a spontaneously immortalized human breast epithelial cell line, MCF-10. Cancer Res *50*, 6075-6086.

Stacker, S. A., Caesar, C., Baldwin, M. E., Thornton, G. E., Williams, R. A., Prevo, R., Jackson, D. G., Nishikawa, S., Kubo, H., and Achen, M. G. (2001). VEGF-D promotes the metastatic spread of tumor cells via the lymphatics. Nature Med *7*, 186-191.

Takanami, I. (2003). Overexpression of CCR7 mRNA in nonsmall cell lung cancer: correlation with lymph node metastasis. Int J Cancer *105*, 186-189.

Takeuchi, H., Fujimoto, A., Tanaka, M., Yamano, T., Hsueh, E., and Hoon, D. S. (2004). CCL21 chemokine regulates chemokine receptor CCR7 bearing malignant melanoma cells. Clin Cancer Res *10*, 2351-2358.

Uchimura, K., Morimoto-Tomita, M., Bistrup, A., Li, J., Lyon, M., Gallagher, J., Werb, Z., and Rosen, S.D. (2006). HSulf-2, an extracellular endosulfatase, is secreted by MCF-7 breast carcinoma cells and selectively mobilizes heparin-bound VEGF, FGF-1, and SDF-1. FASEB J *20*, A1364-A1364.

Van Trappen, P. O., and Pepper, M. S. (2002). Lymphatic dissemination of tumour cells and the formation of micrometastases. Lancet Oncol *3*, 44-52.

Wang, J., Zhang, X., Thomas, S. M., Grandis, J. R., Wells, A., Chen, Z. G., and Ferris, R. L. (2005). Chemokine receptor 7 activates phosphoinositide-3 kinase-mediated invasive and prosurvival pathways in head and neck cancer cells independent of EGFR. Oncogene *24*, 5897-5904.

Weigelt, B., Wessels, L. F., Bosma, A. J., Glas, A. M., Nuyten, D. S., He, Y. D., Dai, H., Peterse, J. L., and van't Veer, L. J. (2005). No common denominator for breast cancer lymph node metastasis. Br J Cancer *93*, 924-932.

Wiley, H. E., Gonzalez, E. B., Maki, W., Wu, M. T., and Hwang, S. T. (2001). Expression of CC chemokine receptor-7 and regional lymph node metastasis of B16 murine melanoma. J Natl Cancer Inst *93*, 1638-1643.

Williams, C. S., Leek, R. D., Robson, A. M., Banerji, S., Prevo, R., Harris, A. L., and Jackson, D. G. (2003). Absence of lymphangiogenesis and intratumoural lymph vessels in human metastatic breast cancer. J Pathol *200*, 195-206.

Wong, S. Y., Haack, H., Crowley, D., Barry, M., Bronson, R. T., and Hynes, R. O. (2005). Tumor-secreted vascular endothelial growth factor-C is necessary for prostate cancer lymphangiogenesis, but lymphangiogenesis is unnecessary for lymph node metastasis. Cancer Res *65*, 9789-9798.

Yucel, G., and Small, S. (2006). Morphogens: precise outputs from a variable gradient. Curr Biol *16*, R29-31.

Zigmond, S. H. (1977). Ability of polymorphonuclear leukocytes to orient in gradients of chemotactic factors. J Cell Biol *75*, 606-616.

Figure legends

Figure 1. 3D tissue culture model of the tumor-lymphatic microenvironment

A: Schematic of the tumor microenvironment where lymphatic vessels drain interstitial fluid, creating interstitial flow directed towards the lymphatic. This fluid convection promotes the transport of signals from tumor to lymphatic, but counteracts diffusive transport of signals from lymphatic to tumor, such as lymphocyte homing chemokine CCL21. The potential role of CCR7 mediated autologous chemotaxis in this process is investigated here along with paracrine CCR7 signaling by lymphatics.

B: Tissue culture model system incorporating a 3D extracellular matrix and interstitial flow to examine cross-talk between tumor cells and lymphatic endothelial cells (LECs) as well as the effects of flow on tumor cell migration, with and without LECs. Inset: Histological cross-section showing interface of tumor suspension, porous membrane, and LECs (arrowheads). Arrows indicate transmigrating tumor cells in membrane pores.

C: Confocal image of the underside of the transwell membrane showing the lymphatic endothelial cell monolayer (CD31, *red*), one adhering tumor cell (GFP, *green*, arrowhead), and one tumor cell in the process of transmigration through a pore (arrow). Nuclei are shown in blue. Bar = 20μm.

D: Human dermal microvascular LECs as characterized by immunofluorescence for indicated markers. Bars = 100μm.

E**:** Flow cytometry of LECs for the markers VE-cadherin, CD31, and podoplanin (negative controls included no primary or secondary antibody, total mouse IgG, and secondary antibody only (AlexaFluor goat anti-mouse 488)).

Figure 2. Tumor cell characterization for CCR7 expression and functional response

A: Immunofluorescence demonstrated CCR7 receptor expression in the three tumor cell lines, but very little in LECs or the non-tumorigenic cell line MCF10A. Bar = 50μm.

B: Representative Western blot analysis of CCR7 expression is qualitatively consistent with immunofluorescence.

C: Relative amounts of CCR7 expression from densitometry of Western blots (n=3), normalized to cell number.

D-**G**: Chemotaxis toward a 4ng/ml/μm gradient of CCL21in 3D matrices of the four mammary cell lines tested. MCF10A cells displayed a small but insignificant response to the CCL21 gradient, while the three tumor cell lines displayed substantial chemotaxis that could be abolished with neutralizing antibodies against CCL21 and CCR7.

H: Summary of CCR7-mediated chemotaxis from the four cell lines, indicating that the more invasive cell lines (ZR-75-1 and MDA-MB-435S) had a stronger chemotactic response to CCL21 than did MCF7 or MCF10A cells. *$p<0.05$; **$p<0.01$compared with control (random migration in basal medium). $^{\Delta}p<0.05$; $^{\Delta\Delta}p<0.01$ between other groups as indicated.

Figure 3. Autocrine secretion of CCR7 ligands by tumor cells

A: Immunostaining for CCL21 and CCL19 (green) in all cell lines after 24 h culture in a 3D matrigel matrix. Nuclei shown in blue; bar = 50μm.

B: CCL21 secretion by each cell type after 24 h culture in 3D matrigel as assessed by ELISA show that in all cases, CCL21 was mostly bound to the matrix, and that the two invasive cell lines, ZR-75-1 and MDA-MB-435S, produced more CCL21 overall than did the other cells.

C: CCL19 secretion as assessed by ELISA showed greater variability than CCL21 secretion, and smaller differences between the different cell lines.

D: Comparison of total CCR7 ligand secreted by cells in 2D vs. 3D culture demonstrates substantially higher secretion rates of CCL21 and CCL19 in 3D culture for all cell lines tested, indicating the importance of microenvironment on chemokine signaling between tumor cells and lymphatics. *$p<0.05$; **$p<0.01$compared with control (random migration in basal medium). $^{\Delta}p<0.05$; $^{\Delta\Delta}p<0.01$ between other groups as indicated.

Figure 4. Tumor cell chemotaxis towards LECs is CCR7-mediated

A-D: Chemotaxis through a 3D matrix of each cell type towards LECs with and without CCR7 blocking antibody cocktail (LEC and LEC block) as compared to basal conditions (no LEC) with or without blocking antibody. **A:** MCF10A, which showed little CCR7 expression, was mildly chemotactic towards LECs, although in a CCR-7-independent manner. **B**: MCF7, which showed higher CCR7 expression than MCF10A but responded weakly to an imposed CCL21 gradient, also showed a small but statistically insignificant 3D chemotaxis towards LECs. **C, D**: both ZR-75-1 and MDA-MB-435S cells were strongly chemoattracted to LECs and their chemotaxis was blocked with anti-CCR7 blocking.

E: Comparing chemotactic responses in 3D, the more invasive cell lines ZR-75-1 and MDA-MB-435S were statistically more chemotactic towards LECs than the benign cell line MCF10A. *$p<0.05$ compared with no LEC basal conditions; $^{\Delta}p<0.05$ between other groups as indicated.

Figure 5. Autologous tumor cell chemotaxis by interstitial flow is CCR7-dependent

A-D: Autologous chemotaxis of each cell type, cultured without LECs, in the direction of 0.2 μm/s interstitial flow, with and without CCR7 blocking antibody cocktail as compared to static conditions. In all cases, CCR7 blocking did not affect baseline (static) migration rates. **A:** The 3D migration of MCF10A cells, which showed little CCR7 expression, doubled in the presence of flow, but was unaffected by CCR7 blocking. **B**: MCF7, which showed higher CCR7 expression than MCF10A but responded weakly to an imposed CCL21 gradient, was three times more migratory in the flow direction than under static conditions; this could be reversed by CCR7 blocking. **C, D**: Migration of both ZR-75-1 and MDA-MB-435S cells increased dramatically under 0.2 μm/s interstitial flow, and this increase was reversed by CCR7 blocking. **E**: Comparison of autologous chemotactic responses among the cell lines shows significant increasing responses according to cell invasiveness: MCF10a < MCF7 < ZR-75-1 < MDA-MB-435S. *$p<0.05$; **$p<0.01$ compared with static conditions; $^{\Delta}p<0.05$; $^{\Delta\Delta}p<0.01$ between other groups as indicated.

Figure 6. Polarization of cells in response to biophysical and biochemical stimuli

A-D: PHAKT-eGFP localization and polarization within ZR-75-1 cells in representative images from **(A)** 3D static gels, **(B)** 3D gels under interstitial flow, **(C)** 3D gels with an exogenous 1% transcellular CCL21 protein gradient, and **(D)** the same CCL21 gradient in 2D culture. Scale bar, 50μm. Insets indicate examples of quantification for representative cells. Arrows illustrate direction of flow (B) or CCL21 gradient (C); for cells in static conditions, one arbitrary direction was fixed as the reference direction.

E: Criteria for quantifying polarization responses of cells. Each cell was scored according to its orientation relative to the direction of flow or imposed CCL21 gradient and assigned as not

polarized or polarized in one of three regions (directed parallel (I), orthogonal (II), or opposite (III) to the direction of flow) as shown.

F: Summary of cell polarization in response to flow (n=34 static, n=58 flow) and CCL21 protein gradients (n=26). In all cases, roughly half or more of analyzed cells were not polarized. Among those cells that did polarize, PHAKT-eGFP localization was directionally unbiased in static conditions, in contrast to conditions of flow and exogenous CCL21 gradient, where cells preferentially polarized with rather than against the direction of flow or exogenous chemotactic gradient.

Figure 7. Combined effects and computational modeling

A: Summary of *in vitro* migration experiments comparing the individual and combined effects of LECs, interstitial flow, and CCR7/CCL21 blocking on transmembrane migration of MDA-MB-435S cells demonstrate that both autocrine and paracrine signaling are CCR7 dependent, and that the combined effect is stronger than each individual effect.

B: Computed transcellular chemokine and enzyme gradients are consistent with *in vitro* migration trends: first, that both LECs (in static conditions) and interstitial flow (in LEC-free conditions) impose the same migratory response in tumor cells, and second, that the combined effect is nearly 3 times larger than that for LECs or interstitial flow alone. Hashed bars represent transcellular enzyme gradients that may potentially cause a secondary effect of directed proteolysis that could explain above-baseline migration levels that persist in flow conditions even with the use of blocking antibodies.

C: Graphical representation of CCL21/19 gradients around a tumor cell embedded in 3D matrix corresponding to (L-R) static culture with LECs, interstitial flow without LECs, and interstitial

flow with LECs. Red-blue color gradient indicates maximal to zero concentration, and arrow indicates direction of flow.

D: Numerical results tabulated for direct comparison.